

Unmasking the Chameleons: A Benchmark for Out-of-Distribution Detection in Medical Tabular Data

Mohammad Azizmalayeri ¹
 Ameen Abu-Hanna ¹
 Giovanni Ciná ^{1,2,3}

M.AZIZMALAYERI@AMSTERDAMUMC.NL
 A.ABU-HANNA@AMSTERDAMUMC.NL
 G.CINA@AMSTERDAMUMC.NL

¹Department of Medical Informatics, Amsterdam Public Health Research Institute, Amsterdam UMC, University of Amsterdam, Netherlands.

²Institute of Logic, Language and Computation, University of Amsterdam, Netherlands.

³Pacmed, Amsterdam, Netherlands.

Abstract

Despite their success, Machine Learning (ML) models do not generalize effectively to data not originating from the training distribution. To reliably employ ML models in real-world healthcare systems and avoid inaccurate predictions on out-of-distribution (OOD) data, it is crucial to detect OOD samples. Numerous OOD detection approaches have been suggested in other fields - especially in computer vision - but it remains unclear whether the challenge is resolved when dealing with medical tabular data. To answer this pressing need, we propose an extensive reproducible benchmark to compare different methods across a suite of tests including both near and far OODs. Our benchmark leverages the latest versions of eICU and MIMIC-IV, two public datasets encompassing tens of thousands of ICU patients in several hospitals. We consider a wide array of density-based methods and SOTA post-hoc detectors across diverse predictive architectures, including MLP, ResNet, and Transformer. Our findings show that i) the problem appears to be solved for far-OODs, but remains open for near-OODs; ii) post-hoc methods alone perform poorly, but improve substantially when coupled with distance-based mechanisms; iii) the transformer architecture is far less overconfident compared to MLP and ResNet.

Keywords: Out-of-Distribution Detection, Medical Tabular Data

1. Introduction

The utilization of ML models in health-related applications is rapidly increasing (Greener et al., 2022;

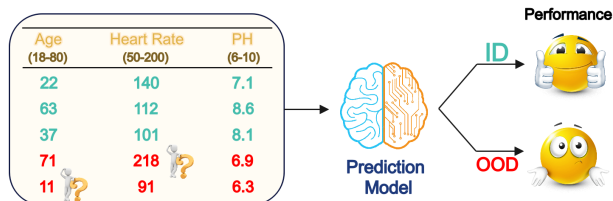


Figure 1: The practical dilemma of OOD data: there are no guarantees on how a model will perform on OOD data, hence real-time OOD detection becomes imperative.

Varoquaux and Cheplygina, 2022). However, a significant limitation lies in their performance evaluation, which is primarily based on optimizing the algorithms for data from the training distribution. This means that they may fail under distribution shift: a model trained on the data from a hospital may not generalize to other hospitals (Rios and Abu-Hanna, 2021; de Hond et al., 2023). Since such ML models are meant to be deployed in real-world healthcare scenarios, ensuring their reliability becomes of utmost importance. One way to prevent models from providing unreliable suggestions is to detect OOD samples in real time, prior to generating predictions. This is known as OOD detection, where a model trained on an in-distribution (ID) set is employed for distinguishing OOD samples from ID data.

In this paper, we investigate this problem for tabular medical data. The problem has already been investigated mainly in the field of computer vision (Yang et al., 2021; Zimmerer et al., 2022), but the results may not extend to tabular medical data. For example, while computer vision has focused on im-

proving post-hoc OOD detectors (Yang et al., 2022), it is demonstrated that these kinds of methods perform even worse than a random classifier in medical tabular data due to the phenomenon of over-confidence (Ulmer et al., 2020; Ulmer and Cinà, 2021; Zadorozhny et al., 2022).

Existing OOD detection methods can be categorized into three main groups: i) post-hoc methods, which are detectors that can be applied on top of any trained classifier, such as Maximum Softmax Probability (MSP) (Hendrycks and Gimpel, 2017), ii) density-based methods, which are trained to estimate the marginal distribution of the training set in order to detect samples that fall out of the training distribution, such as auto-encoders (AEs) (Kingma and Welling, 2014), and finally iii) methods that require retraining of the prediction model which are mainly designed specifically to be applied on images, such as OpenGAN (Kong and Ramanan, 2021).

The focus of this work is medical tabular data, thus we only consider the first two OOD categories since they can be applied to any medical tabular dataset without limitations. Furthermore, we examine three important architectures for the classifier on which post-hoc methods are implemented, namely MLP, ResNet, and FT-Transformer (Gorishniy et al., 2021)—to assess their impact on OOD detection.

A crucial aspect of comparing these methods involves evaluating their performance across diverse scenarios. Therefore, we incorporate the latest publicly available datasets including eICU and MIMIC-IV (Pollard et al., 2018; Johnson et al., 2023) in our experiments. We also employ different approaches for classifying the data into ID and OOD sets. This lets us consider OOD sets near to and far from the IDs in the experiments, which are referred to as near-OOD and far-OOD (Fort et al., 2021). For example, to consider near-OOD instances, the ID and OOD sets can be constructed by dividing a dataset based on a distinguishing feature such as gender (male vs. female), and for a far-OOD experiment, we can use a dataset from a different data generating process, such as a distinct care protocol (de Hond et al., 2023), or generate artificial OOD samples.

We use this setup to conduct broad experiments that can illustrate the differences between various types of OOD detection methods in order to provide the community with an extensive reproducible benchmark in the medical tabular data domain¹. Our re-

sults are provided in section 5, and the main findings are as follows: i) the OOD detection problem appears to be almost resolved on far-OOD samples, but it is still an open issue for near-OODs, ii) the distance-based post-hoc OOD detectors are better than other post-hoc methods, iii) unlike the claims in previous work, post-hoc methods can be competitive with the density-based ones, iv) the transformer architecture mitigates the problem of over-confidence that other models suffer from.

2. Related Work

OOD detection has received a lot of attention, with several kinds of approaches being proposed for this purpose. This has resulted in interest in comparing these methods fairly within the same setting. Some benchmarks compare methods using standard image datasets (Han et al., 2022; Yang et al., 2022; Zhang et al., 2023a). However, it is still necessary to have benchmarks that are specific to other domains and data modalities. For example, the MOOD challenge (Zimmerer et al., 2022) investigated OOD detection within the context of medical imaging, with various new methods showing outstanding results (Marimont and Tarroni, 2021; Tan et al., 2022).

In the realm of medical tabular datasets, notable endeavors have been undertaken. A pipeline is presented in Nicora et al. (2022) to train a model on ICU data and detect test samples for which the model might exhibit poor performance. BEDS-Bench (Avati et al., 2021) has provided a benchmark on the generalization ability of ML models over electronic health records, highlighting performance drops under distribution shift. Moreover, it has been found that access to OOD data does not improve the test performance on ICU data (Spathis and Hyland, 2022). The work by Ulmer et al. (2020), proposed one of the first comparisons between basic OOD detectors in the space of medical tabular data, pointing to the fact that the problem of OOD detection was wide open. Also, some guidelines have been provided on how to evaluate an OOD detector in practice within the context of medical data (Zadorozhny et al., 2022) such as methods for selecting the OOD set during evaluation. Compared to this related work, we benchmark the most recent SOTA OOD detection approaches and SOTA architectures, leading to novel insight e.g. on the over-confidence of transformers and the combination of post-hoc and distance-based methods.

1. The codes are available at <https://github.com/mazizmalayeri/TabMedOOD>.

3. Problem Definition and Evaluation Protocol

In the following, we describe the problem definition, the metrics used to measure performance, and how we select the ID and OOD sets.

3.1. OOD Detection

In training any ML model, we require a training set $\mathcal{D}_{in} = \{(x_i, y_i)\}_{i=1}^n$, where each instance x_i has a label y_i . Our goal is to have a model $f : \mathcal{X} \rightarrow \mathcal{R}$ and a binary classifier $G_\lambda : \mathcal{X} \rightarrow \{0, 1\}$ such that for a test input $x \sim \mathcal{X}$:

$$G_\lambda(x; f) = \begin{cases} \text{OOD} & f(x) \geq \lambda \\ \text{ID} & f(x) < \lambda \end{cases}. \quad (1)$$

The score according to f is sometimes called the ‘novelty score’. Samples whose novelty score is higher than the threshold λ are classified as OOD. Hence, the final goal would be to train model f such that it assigns lower scores to $x \sim \mathcal{D}_{in}$ and higher scores to $x \sim \mathcal{D}_{out}$, where \mathcal{D}_{out} is the dataset that includes the OOD samples.

3.2. Metrics

To assess the separability of the ID and OOD scores given by f , we measure the area under the receiver operating characteristic (AUROC) as a well-known threshold-independent classification criterion, and FPR@95, which measures the FPR at a λ corresponding to the TPR being equal to 95%.

3.3. Near, Far, and Synthesized OOD

The distance between \mathcal{D}_{in} and \mathcal{D}_{out} plays an important role in the performance of OOD detection methods. It is relatively simpler to detect samples far from the training distribution than samples close to it; we refer to the former samples as far-OOD and to the latter as near-OOD. To consider this in the comparisons, we define different sets of ID and OOD as follows.

Near and far OODs: Assuming that we have a dataset \mathcal{D} , we can define the ID and OOD sets in two ways: First, we can separate \mathcal{D} based on a specific feature such as gender (male vs. female) or age (e.g. elderly vs. young). This reflects what may happen when employing an ML model in practice. As an example, if one develops a model on a population of mostly young people, it might not be fully reliable

when applied to the elderly. The second way would be to use \mathcal{D} as ID and a totally different dataset as OOD. Since identifying OODs in the second scenario appears to be easier, we will refer to the first scenario as near-OOD and the second as far-OOD following the convention in computer vision (Winkens et al., 2020; Fort et al., 2021).

Synthesized-OOD: Following the data corruption suggested in Ulmer et al. (2020), we can simulate the OOD samples by scaling a single feature from ID set by a factor of 10, 100, or 1000. For each factor, we will repeat the experiments 100 times with different features, and average the results to isolate the influence of scaling in the results, minimizing the impact of the chosen feature. By increasing the scaling factor, it looks like we are gradually transforming near-OOD samples into far-OOD ones.

4. Experiment Setup

4.1. Supported OOD Detectors

Two main OOD detection method categories, described in Table 1, are included in our experiments. The first category is density estimators, which learn the marginal distribution of the ID data and label OOD samples by comparison to such distribution. We include 7 density-based models covering different types of density estimators. These methods are used in prior works and have reached outstanding results (Ulmer et al., 2020; Zadorozhny et al., 2022).

The second group is the post-hoc detectors, which can be integrated into any pre-trained classifier without requiring any additional fine-tuning or training. They mostly generate a novelty score for the input based on the classifier output or intermediate representations. We evaluate 17 different post-hoc detectors, including both commonly used detectors and top-performing ones in their respective fields.

4.2. Datasets

We use eICU (Pollard et al., 2018) and MIMIC-IV (Johnson et al., 2023) in our experiments as two public and popular datasets encompassing tens of thousands of ICU patients in several hospitals. Following the descriptions in section 3.3, each of these datasets is considered as far-OOD set for the other one. For the near-OOD case, we divide the datasets based on the time-independent variables, as this choice better emulates the potential distribution shifts in ID data

Method	Short Description
AE, VAE (Kingma and Welling, 2014)	Encodes input in a latent representation and reconstructs it.
HI-VAE (Nazabal et al., 2020)	Modifies VAE to consider heterogeneous data.
Flow (Papamakarios et al., 2017)	Estimates ID data by transformations into a normal distribution.
PPCA (Tipping and Bishop, 1999)	Reduces data dimensionality based on singular value decomposition.
LOF (De Vries et al., 2010)	Compares local density of input to the density of its closest neighbors.
DUE (van Amersfoort et al., 2021)	Uses a deep neural Gaussian process for modeling the ID data.
MDS (Lee et al., 2018)	Uses Mahalanobis distances to the class-conditional normal distributions.
RMDS (Ren et al., 2021)	Modifies MDS for detecting near-OODs.
KNN (Sun et al., 2022)	Measures distance of input to the k_{th} nearest neighbor in the ID data.
VIM (Wang et al., 2022)	Uses logits and features norm simultaneously.
SHE (Zhang et al., 2023b)	Measures the distance of input to the class-conditional representations.
KLM (Hendrycks et al., 2022)	Uses KL distance of softmax output from its range over the ID data.
OpenMax (Bendale and Boult, 2016)	Fits a Weibull distribution on the logits instead of softmax.
MSP (Hendrycks and Gimpel, 2017)	Uses maximum softmax probability as a simple but effective baseline.
MLS (Hendrycks et al., 2022)	Uses the maximum logit score instead of MSP.
TempScale (Guo et al., 2017)	Calibrates the temperature parameter in the softmax.
ODIN (Liang et al., 2018)	Perturbs the input adversarially before using TempScaling.
EBO (Liu et al., 2020)	Uses an energy function instead of softmax.
GRAM (Sastry and Oore, 2020)	Measures deviation of the Gram matrix from its range over the ID data.
GradNorm (Huang et al., 2021)	Uses norm of the backpropagated gradients.
ReAct (Sun et al., 2021)	Rectifies the model activations at an upper limit.
DICE (Sun and Li, 2022)	Suggests sparsification of the last linear layer.
ASH (Djurisic et al., 2023)	Extends the DICE idea to the intermediate feature layers.

Table 1: Density-based models and post-hoc detectors evaluated in this work, with a short description.

that can be encountered in practice than the time-dependent ones. Among the time-independent variables available for each dataset, we have selected age (older than 70 as ID), gender (females as ID), and ethnicity (Caucasian or African American as ID) in eICU, and Age (older than 70 as ID), gender (females as ID), admission type (surgical in the same day of admission as ID), and first care unit (CVICU as ID) in MIMIC-IV dataset. In each case, the remaining part of the dataset would be OOD. The results for the age (older than 70), ethnicity (Caucasian), and first care unit (CVICU) are reported in the main text, and others in Appendix C.

4.3. Pre-processing

We pre-processed the eICU data using the pipeline provided in Sheikhalishahi et al. (2020). Subsequently, the data is filtered to keep only patients with a length of stay of at least 48 hours and an age greater than 18 years old. Additionally, data with unknown discharge status were removed. Furthermore, patients with NaN values in the features used in our models are also removed. This pre-process resulted in a total 54826 unique patients for this dataset.

For the MIMIC-IV, we used the pipeline provided in Gupta et al. (2022) with slight modifications e.g.,

we added a mapping from the feature IDs to feature names to have each feature name in the final pre-processed data. The data is then filtered similarly to the eICU dataset. This resulted in 18180 unique patients for this dataset.

These datasets contain different types of clinical variables, but they are not recorded for all the patients. To avoid NaN values as much as possible, we are interested in using only the more important variables that are recorded for more patients. Based on these criteria and considering the important clinical variables suggested in Ulmer et al. (2020), we have selected a combination of time-dependent and time-independent variables for each dataset, which are reported in Appendix A.

It should be noted that when datasets are evaluated against each other, only the variables found in both datasets are taken into account. Moreover, for the time-dependent variables, we aggregated the time series by means of 6 different statistics including mean, standard deviation, minimum, maximum, skewness, and number of observations calculated over windows consisting of the full time-series and its first and last 10%, 25%, and 50%.

4.4. Task and Prediction Models

To perform post-hoc OOD detection, we would need a prediction model performing a supervised classification task. The main task that is used in prior work is mortality prediction (Sheikhalishahi et al., 2020; Ulmer et al., 2020; Meijerink et al., 2020; Zadorozhny et al., 2022). In mortality prediction, we only use the first 48 hours of data from the intensive care unit collected from patients to predict the in-hospital mortality. It is noteworthy that the mortality rate in the pre-processed data is 12.57% in the MIMIC-IV and 6.77% in the eICU dataset.

To perform this task, we consider three widely used architectures: MLP, ResNet, and FT-Transformer (Gorishniy et al., 2021). MLP passes data through the fully-connected layers and non-linear activation functions with dropout to improve the generalization. ResNet adds batchnorm and residual connections to MLP. We also consider FT-Transformer, constituted of transformer blocks that utilize the attention mechanism (Vaswani et al., 2017).

5. Results

In this section, we describe the results for each of the OOD settings based on the AUROC criterion. Results for FPR@95 are presented in Appendix D. Moreover, each experiment is repeated 5 times, and the results are averaged to reduce the impact of randomness in selecting train/test data and training itself. Additionally, we have measured the mortality prediction performance of the prediction models in Appendix B, indicating that they are trained well.

5.1. Far-OOD

Results for the far-OOD setting are displayed in Table 2. According to this table, there are methods that can effectively detect OOD data on each dataset.

Among the density-based methods, Flow attains the best result on eICU, while others exhibit superior performance on MIMIC-IV. Additionally, DUE can detect OODs on MIMIC-IV, but it falls short of being competitive on the eICU dataset. Except for these two approaches and HI-VAE, other density-based methods including AE, VAE, PPCA, and LOF demonstrate strong performance on both datasets.

Within the post-hoc methodologies, MDS exhibits better results compared to others regardless of the choice of the prediction model. Moreover, MDS applied on ResNet is competitive with the density-based

approaches, even marginally outperforming them based on the average results across both datasets. After MDS, there is not a single winner. However, approaches like KNN, VIM, and SHE which somehow compute the distance to the training set as the novelty score, outperform the rest.

Regarding the prediction model, the top-performing methods on ResNet demonstrate superior results compared to both MLP and FT-Transformer. However, a problem with ResNet and MLP is that they have over-confidence issues with some approaches on MIMIC-IV. This means that they have more confidence in the OODs, resulting in a performance even worse than a random detector. This is mainly being observed with the detectors that do not rely on distance-based novelty scores such as MSP and GradNorm. Note that the eICU dataset contains data from a more extensive array of hospitals, which can increase diversity in the data and reduce the over-confidence on this dataset.

FT-Transformer seems to solve the over-confidence problem observed in MLP and ResNet, as all detectors perform better than random on both datasets. The attention mechanism in the transformer blocks enables this model to consider relationships between input elements, leading to a better understanding of ID data.

5.2. Near-OOD

Results for the near-OOD setting are presented in Table 2. In the eICU dataset, the diversity among the ID data and the proximity of OODs to ID have collectively yielded an almost random performance for all the approaches. Still, it indicates that methods like MDS and Flow are marginally better than others.

In MIMIC-IV, which contains less diversity, the age variable still results in an almost random performance across all approaches, but FCU reflects some differences between detectors. Among the density-based approaches, AE and VAE are the best choices, followed by PPAC, LOF, and HI-VAE. The post-hoc methods mostly demonstrate similar performance within the same architecture category. Moreover, they can be competitive with density-based methods when applied on the FT-Transformer.

5.3. Synthesized-OOD

Results for the synthesized-OOD setting are displayed in Table 3. It is expected that increasing the

Model	Method	eICU			MIMIC-IV		
		Far-OOD	Near-OOD(Eth)	Near-OOD(Age)	Far-OOD	Near-OOD(FCU)	Near-OOD(Age)
Density Based	AE	96.5±0.2	55.1±0.8	50.0±0.4	99.8±0.0	79.4±0.6	56.8±0.4
	VAE	95.8±0.2	55.4±0.7	50.1±0.4	99.8±0.0	79.7±0.6	57.0±0.4
	HI-VAE	56.7±1.6	44.3±1.2	44.4±2.1	68.8±8.8	79.1±13.4	56.8±10.0
	Flow	100.0±0.0	61.1±0.9	49.7±0.4	87.4±7.5	31.8±3.9	51.6±0.5
	PPCA	96.7±0.2	59.1±0.6	51.3±0.5	99.8±0.0	75.1±0.6	56.8±0.7
	LOF	96.5±0.1	56.0±0.8	49.5±0.5	99.2±0.2	73.5±0.5	55.3±0.8
	DUE	73.4±0.5	53.7±0.9	49.5±0.4	98.2±0.2	59.8±1.7	51.6±0.6
MLP	MDS	84.3±1.4	56.8±0.9	51.7±0.7	98.9±0.6	68.0±3.9	53.8±0.9
	RMDS	59.2±2.1	50.0±1.7	49.1±0.5	79.9±12.1	60.9±1.1	50.5±0.4
	KNN	79.4±1.2	53.4±2.4	48.5±0.8	65.4±8.3	73.3±0.9	54.0±0.5
	VIM	69.9±1.4	51.2±1.7	46.7±0.8	97.8±2.4	71.1±1.2	54.0±0.9
	SHE	61.5±0.8	50.8±1.9	50.1±0.1	93.9±5.7	56.7±0.7	49.6±0.2
	KLM	56.8±1.2	52.7±1.8	51.7±0.2	79.5±5.8	46.1±2.0	49.3±0.6
	OpenMax	52.1±1.3	47.4±1.5	46.3±1.3	62.7±10.3	66.9±0.9	52.6±0.5
	MSP	51.2±1.2	47.1±1.8	46.3±1.3	13.4±7.7	66.0±0.6	52.4±0.4
	MLS	51.3±1.4	46.8±1.7	46.2±1.3	14.2±7.6	65.9±0.8	52.3±0.4
	TempScale	51.2±1.2	46.8±1.8	46.3±1.3	13.3±7.7	66.0±0.8	52.4±0.3
	ODIN	51.3±1.2	46.8±1.8	46.3±1.3	13.5±7.8	65.9±0.8	52.5±0.3
	EBO	51.4±1.4	46.8±1.7	46.2±1.3	14.4±7.7	65.9±0.8	52.3±0.4
	GRAM	46.7±1.4	46.6±1.5	48.4±0.6	16.7±11.7	53.6±4.1	49.9±0.1
	GradNorm	50.2±1.3	46.8±1.8	46.4±1.3	12.7±7.9	65.8±0.8	52.5±0.4
ReAct	52.5±1.2	46.7±1.5	46.6±1.4	74.3±19.6	66.1±0.9	52.5±0.4	
DICE	50.6±1.3	46.9±1.8	46.6±1.3	14.7±8.4	65.8±0.9	52.7±0.8	
ASH	50.6±1.3	46.8±1.5	46.6±1.7	14.0±7.3	65.7±0.9	52.1±0.4	
ResNet	MDS	96.9±0.3	58.4±0.6	51.6±0.7	99.7±0.1	74.0±2.4	55.4±0.3
	RMDS	45.8±2.9	50.1±2.5	49.9±0.3	79.5±13.1	62.6±1.4	50.8±0.4
	KNN	91.2±0.9	59.2±1.6	50.1±0.1	93.0±1.9	57.7±2.3	54.3±0.5
	VIM	93.5±1.0	56.9±1.5	48.2±1.1	99.5±0.2	75.0±1.8	56.2±0.4
	SHE	86.7±1.6	50.5±1.3	51.7±0.8	99.7±0.1	73.0±1.6	52.8±0.6
	KLM	55.5±2.6	47.5±1.5	51.5±0.4	78.1±6.7	55.2±1.4	47.7±0.2
	OpenMax	64.8±5.4	50.7±1.3	47.0±1.1	65.2±24.9	67.2±4.1	54.3±0.4
	MSP	63.6±5.0	51.3±2.4	47.1±0.8	19.5±10.3	65.0±4.3	53.9±0.7
	MLS	64.4±6.0	51.9±2.2	46.8±1.4	38.0±26.5	66.5±4.6	54.1±0.3
	TempScale	63.6±5.0	51.3±2.4	47.1±0.8	19.5±10.3	65.0±4.3	53.9±0.7
	ODIN	63.7±5.0	51.3±2.4	47.1±0.8	19.6±10.4	65.0±4.4	53.9±0.7
	EBO	64.4±6.1	52.0±2.2	46.8±1.4	38.5±27.0	66.5±4.6	54.2±0.3
	GRAM	39.3±2.6	48.6±1.2	49.0±0.9	11.3±5.0	44.2±1.7	49.6±0.1
	GradNorm	48.1±5.6	49.8±1.6	47.5±1.1	7.5±4.8	48.2±6.9	52.7±0.6
ReAct	71.8±3.9	52.7±1.8	47.4±1.5	81.4±9.1	73.9±2.6	55.3±0.4	
DICE	52.9±7.9	50.5±1.2	47.3±0.6	17.0±7.6	57.7±7.4	55.5±0.5	
ASH	68.1±5.6	51.5±2.4	47.2±0.8	40.5±27.9	63.9±4.3	53.9±0.5	
FT-T	MDS	84.1±4.2	58.5±2.2	50.8±1.1	94.2±0.7	77.8±2.0	50.1±0.2
	RMDS	57.3±0.9	51.6±1.5	48.3±0.7	75.8±13.5	60.6±4.4	50.9±1.5
	KNN	85.5±3.7	55.8±1.9	49.6±0.2	92.0±0.6	78.6±3.2	51.7±1.5
	VIM	85.5±2.8	57.3±2.3	48.8±0.1	96.8±0.7	79.4±1.7	53.8±0.3
	SHE	62.9±1.3	50.5±1.7	50.4±0.7	85.2±9.1	67.5±0.5	47.1±0.5
	KLM	52.0±2.1	51.6±2.1	51.0±0.7	74.8±6.0	49.3±2.6	47.3±1.1
	OpenMax	74.3±2.4	48.7±0.8	48.1±0.5	66.5±8.3	77.7±3.5	53.5±0.2
	MSP	74.3±2.5	48.4±1.0	48.1±0.5	66.1±7.6	77.6±3.7	53.4±0.2
	MLS	74.1±2.5	49.1±1.1	48.0±0.5	65.2±6.4	77.8±3.2	53.3±0.2
	TempScale	74.3±2.5	48.4±1.0	48.1±0.5	66.1±7.6	77.6±3.7	53.4±0.2
	ODIN	74.4±2.4	48.4±1.0	48.1±0.5	66.3±7.5	77.6±3.7	53.4±0.2
	EBO	74.1±2.4	49.1±1.1	48.0±0.5	64.4±5.9	77.8±3.1	53.3±0.3
	GRAM	73.5±2.3	50.8±2.7	48.6±0.6	70.0±6.8	75.2±5.4	51.7±0.4
	GradNorm	69.5±5.9	50.4±3.4	48.7±0.8	66.4±6.8	62.5±8.9	53.1±0.5
ReAct	73.9±2.6	48.1±1.1	48.2±0.7	64.0±4.3	77.8±2.6	53.4±0.3	
DICE	74.3±2.2	49.9±2.8	48.1±0.6	77.7±7.1	77.3±4.1	53.2±0.6	
ASH	73.0±3.2	52.6±2.7	48.6±1.3	58.0±8.5	75.4±3.4	52.5±1.1	

Table 2: Comparing OOD detection methods in the *far-OOD* and *near-OOD* settings using eICU and MIMIC-IV datasets, with performance evaluated through AUROC. The name in the top row shows the dataset considered as ID in the far-OOD experiment and divided for the near-OOD test. FCU and Eth stand for first care unit and ethnicity as the variables utilized for constructing the ID/OOD sets. Results are averaged over 5 runs. For each model, the best value in each column is shown in bold, and distance-based post-hoc approaches are distinguished with a lighter color.

Model	Method	eICU			MIMIC-IV		
		$\mathcal{F}=10$	$\mathcal{F}=100$	$\mathcal{F}=1000$	$\mathcal{F}=10$	$\mathcal{F}=100$	$\mathcal{F}=1000$
Density Based	AE	80.5±1.3	88.4±0.9	90.0±0.7	76.4±1.6	83.9±2.1	86.6±2.1
	VAE	80.0±1.3	88.3±0.9	89.9±0.7	76.4±1.6	83.8±2.1	86.6±2.1
	HI-VAE	50.0±0.1	50.0±0.1	50.1±0.2	50.59±0.8	51.3±1.4	52.0±2.0
	Flow	70.2±2.5	82.1±2.5	87.7±1.4	53.8±1.8	65.0±3.0	75.7±2.5
	PPCA	80.7±1.3	88.3±0.9	89.7±0.8	76.9±1.5	84.0±2.1	86.6±2.0
	LOF	84.4±1.3	89.4±0.8	90.5±0.7	78.4±1.5	84.7±2.1	86.9±1.9
DUE	63.9±1.6	80.5±1.3	88.7±0.8	60.3±2.2	76.0±1.9	83.0±2.0	
MLP	MDS	68.5±2.4	82.8±2.0	89.2±2.0	69.3±2.4	80.8±1.6	84.7±1.8
	RMDS	60.8±1.0	75.2±2.0	85.8±2.0	52.7±4.1	64.5±6.9	76.4±2.8
	KNN	60.3±1.5	68.0±2.0	70.9±2.3	59.1±4.9	67.2±8.9	70.7±10.0
	VIM	48.5±2.0	47.2±3.1	46.0±4.9	56.8±7.9	63.5±13.7	66.6±15.1
	SHE	62.5±2.8	77.8±1.6	89.8±0.1	62.3±3.0	77.8±2.2	83.6±1.5
	KLM	60.2±1.4	69.6±1.5	78.1±1.4	55.4±2.0	66.9±1.6	74.0±1.5
	OpenMax	52.6±2.0	65.2±2.5	77.4±2.5	48.4±5.3	54.0±5.1	69.4±5.6
	MSP	40.5±2.2	27.1±3.0	14.2±2.4	45.7±4.8	31.7±5.5	21.8±1.3
	MLS	40.4±2.4	27.0±3.4	13.8±2.8	45.6±4.1	32.1±4.0	24.9±3.7
	TempScale	40.4±2.2	27.0±3.1	14.0±2.4	45.7±4.8	31.6±5.5	21.7±1.3
	ODIN	40.5±2.2	27.0±3.1	14.0±2.4	45.7±4.8	31.7±5.5	21.8±1.3
	EBO	40.4±2.4	27.0±3.4	13.8±2.8	45.5±3.9	32.0±4.0	24.9±3.8
	GRAM	38.7±2.0	25.2±2.6	12.7±2.1	47.0±0.7	32.8±3.0	20.4±2.2
	GradNorm	40.2±2.1	26.4±2.9	13.2±2.4	42.6±2.4	26.1±1.1	18.8±1.4
	ReAct	45.0±1.6	37.3±2.7	31.3±2.5	49.0±5.7	46.6±12.4	46.7±14.5
	DICE	40.9±2.7	28.9±3.5	16.7±2.9	44.8±3.6	31.4±2.7	22.0±1.1
ASH	40.4±2.4	27.3±3.1	14.3±2.6	45.3±4.1	32.1±4.3	25.1±3.7	
ResNet	MDS	74.4±2.0	88.9±1.7	91.3±1.4	72.4±1.1	81.8±0.8	85.4±1.0
	RMDS	51.7±0.6	59.8±2.5	78.7±2.4	46.2±1.5	57.6±2.7	73.9±1.2
	KNN	69.5±2.1	84.8±2.2	87.9±2.2	67.5±1.5	79.1±1.2	83.7±0.8
	VIM	72.2±2.5	88.7±1.8	91.5±1.4	68.8±1.3	80.2±1.2	84.5±1.1
	SHE	68.2±0.7	86.6±0.5	91.5±0.2	67.2±1.4	80.0±0.9	84.5±0.7
	KLM	56.6±0.8	69.4±1.7	80.5±1.9	53.2±0.9	65.4±0.5	75.3±0.8
	OpenMax	57.5±0.7	66.4±4.3	77.4±2.9	55.2±1.0	61.6±1.4	61.7±11.4
	MSP	49.4±2.2	35.1±2.1	16.8±1.0	52.2±1.1	38.0±0.7	23.1±0.9
	MLS	49.0±1.7	34.7±2.0	18.5±2.8	52.5±1.9	40.5±7.0	31.0±8.8
	TempScale	49.4±2.2	35.1±2.1	16.8±1.0	52.2±1.1	38.0±0.7	23.1±0.9
	ODIN	49.4±2.2	35.2±2.1	16.8±1.0	52.3±1.1	38.1±0.7	23.1±0.9
	EBO	49.0±1.6	34.5±2.1	18.5±2.8	52.4±2.1	40.6±7.4	31.0±9.0
	GRAM	37.0±3.1	17.7±3.0	9.1±1.6	46.6±1.2	29.0±0.7	18.9±0.9
	GradNorm	40.1±2.4	20.4±1.0	9.7±1.6	44.9±1.0	25.7±0.9	17.2±0.3
ReAct	59.4±1.5	70.4±3.5	74.8±3.5	58.7±2.0	67.2±4.1	70.2±4.4	
DICE	42.6±2.0	24.6±1.2	10.8±0.9	50.6±1.6	36.8±1.6	23.1±1.5	
ASH	49.8±0.3	36.7±2.4	20.1±2.9	52.3±1.7	40.9±5.2	31.1±8.5	
FT-T	MDS	59.9±1.4	79.5±1.4	87.5±0.9	59.7±1.1	76.0±1.2	81.8±1.4
	RMDS	51.5±1.3	57.8±7.4	64.0±13.0	49.0±0.9	55.0±2.0	67.0±5.1
	KNN	57.3±1.4	75.4±2.2	86.5±1.3	57.6±1.2	74.6±1.0	81.4±1.3
	VIM	57.9±1.6	77.6±1.3	88.3±0.7	57.4±2.5	74.3±1.2	80.9±1.2
	SHE	55.7±1.3	71.2±2.9	80.4±1.6	53.2±0.7	67.6±1.6	80.8±2.4
	KLM	54.1±0.8	63.1±1.1	72.1±4.2	52.8±0.4	60.8±1.1	61.8±6.9
	OpenMax	51.0±0.7	56.1±2.7	71.4±3.2	48.8±0.9	54.1±2.6	66.4±3.8
	MSP	50.9±0.6	55.8±2.7	71.3±3.1	48.4±0.8	49.6±1.5	62.9±2.9
	MLS	50.9±0.7	55.8±3.1	70.8±3.1	48.4±0.9	49.5±2.7	60.5±5.6
	TempScale	50.9±0.6	55.8±2.7	71.3±3.1	48.4±0.8	49.6±1.5	62.9±2.9
	ODIN	50.9±0.6	55.9±2.7	71.4±3.1	48.4±0.8	49.7±1.5	63.1±2.9
	EBO	50.9±0.7	55.5±3.1	70.2±3.2	48.5±1.0	49.0±3.4	57.3±7.4
	GRAM	48.9±0.1	50.1±0.8	62.5±3.0	47.8±1.3	44.0±2.7	49.6±7.6
	GradNorm	52.0±0.8	59.5±2.9	73.6±2.9	48.8±0.9	51.4±1.7	64.2±2.7
	ReAct	50.9±0.8	55.7±3.4	69.9±3.2	48.6±1.1	49.7±3.4	57.4±7.1
	DICE	52.2±1.5	62.8±2.5	75.6±1.4	50.2±0.9	64.5±1.4	76.5±1.6
ASH	50.1±1.4	54.6±2.1	69.7±1.3	48.7±0.9	49.9±2.8	59.2±5.6	

Table 3: Comparing OOD detection methods in the *synthesized-ODD* setting using eICU and MIMIC-IV datasets, with performance evaluated through AUROC. In this setting, one feature is multiplied by a specific factor \mathcal{F} to construct an OOD sample. For each model and factor we display the average performance, calculated over 100 resampling of the feature and 5 different initializations of the model. For each model, the best value in each column is shown in bold, and distance-based post-hoc approaches are distinguished with a lighter color.

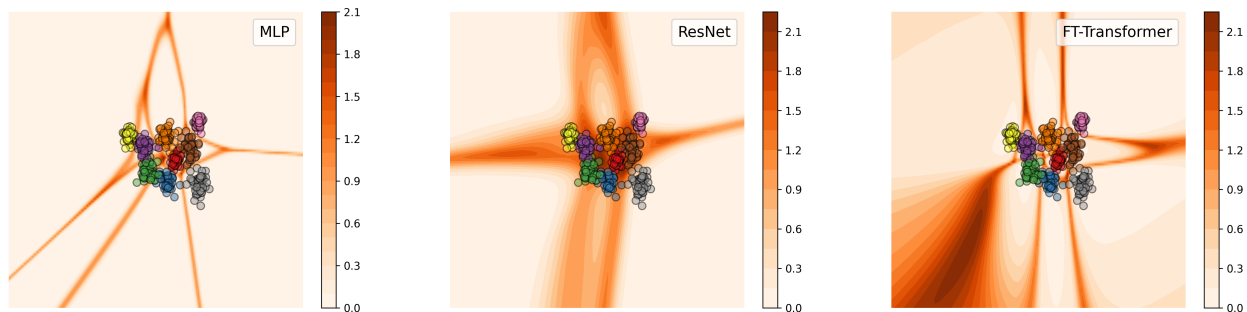


Figure 2: Depiction of confidence scores for different architectures. High confidence (low entropy) is represented in light orange. MLP and ResNet exhibit regions of confidence extending far away from the ID data. FT-Transformer mitigates this over-confidence but does not solve it.

scaling factor (\mathcal{F}) in this setting facilitates the detection of OODs. However, over-confidence hampers OOD detection, causing certain methods to exhibit a totally opposite behavior with MLP and ResNet architectures, on both datasets. In this case, even the diversity in eICU does not prevent over-confidence. Similar to the far-OOD scenario, FT-Transformer seems to solve this issue, as increasing \mathcal{F} results in an improved performance for this architecture.

To compare different approaches, density-based methods like AE, VAE, PPCA, and LOF demonstrate better performance than post-hoc ones when $\mathcal{F} = 10$. However, this gap in performance is reduced with increasing \mathcal{F} to the extent that methods like MDS, VIM, and SHE applied on ResNet are outperforming density-based ones on the eICU dataset with $\mathcal{F} = 1000$.

5.4. Over-confidence

The results above showed over-confidence for the MLP and ResNet architectures, whereas the FT-Transformer appeared as a solution to this problem. For a more visual exploration of this issue, we employ a classification toy example. In this example, each of the predictive architectures is trained on a multi-class classification task with 2D samples. Next, the entropy of the model’s softmax output is plotted for a wide array of inputs. Plots are shown in Fig. 2, with a lighter color indicating more confidence (i.e. low entropy in the softmax output). As depicted in this figure, MLP and ResNet confidence is increased by getting further away from the ID data. This observation validates the presence of over-confidence in both the MLP and ResNet models. Conversely, in

the FT-Transformer, confidence increases along certain directions and decreases in others. This suggests that the transformer can mitigate the over-confidence in some directions, but does not solve it entirely.

6. Discussion

According to our results, when OODs are far from ID data, there exist methods that can effectively perform OOD detection. However, OODs near to ID data such as multiplication by $\mathcal{F} = 10$ or in a near-OOD setting are still challenging to spot. While the poor results in the near-OOD scenarios might be due to a large overlap with the ID data, when multiplying features with a scaling factor one can ensure that there is a clear difference between such OOD and ID data. This points to the fact that there is still ample room for improvement in detecting near OODs.

Delving into OOD detectors, density-based methods, particularly AE, VAE, PPCA, and Flow, exhibit consistent good performance across different settings and datasets. Within the post-hoc methods, they perform poorly in some cases, but they improve substantially and become competitive with the density-based ones when used in conjunction with the distance-based mechanisms. For example, MDS applied on ResNet can even marginally outperform density-based methods in some cases, such as the experiment with a scaling factor of $\mathcal{F} = 1000$ on the eICU dataset. This nuances previous claims that post-hoc methods generally exhibit poor performance (Ulmer et al., 2020; Zadorozhny et al., 2022).

To compare different prediction models, ResNet combined with distance-based detectors demon-

strates better results than MLP and FT-Transformer. On the other hand, MLP and ResNet suffer from over-confidence, causing certain detectors to perform even worse than a random classifier. This aligns with what was highlighted in prior studies (Hein et al., 2019; Ulmer and Cinà, 2021). Our numerical results suggest that FT-Transformer could be a solution to this problem, however, our simple example with toy data showcases that transformers do not completely eliminate over-confidence.

This benchmark is built on two intensive care datasets, which are highly granular. Hence, caution should be exercised when transporting these findings to alternative healthcare tabular datasets with different characteristics. To facilitate the extension of this benchmark, we provided a modular implementation allowing for the addition of new datasets and methods to the experiments.

References

- Anand Avati, Martin Seneviratne, Yuan Xue, Zhen Xu, Balaji Lakshminarayanan, and Andrew M. Dai. BEDS-bench: Behavior of EHR-models under distributional shift - a benchmark. In *NeurIPS 2021 Workshop on Distribution Shifts: Connecting Methods and Applications*, 2021.
- Abhijit Bendale and Terrance E Boult. Towards open set deep networks. In *Proceedings of the IEEE conference on computer vision and pattern recognition*, 2016.
- Anne AH de Hond, Ilse MJ Kant, Mattia Fornasa, Giovanni Cinà, Paul WG Elbers, Patrick J Thoral, M Sesmu Arbous, and Ewout W Steyerberg. Predicting readmission or death after discharge from the icu: external validation and retraining of a machine learning model. *Critical Care Medicine*, 51(2):291, 2023.
- Timothy De Vries, Sanjay Chawla, and Michael E Houle. Finding local anomalies in very high dimensional space. In *2010 IEEE International Conference on Data Mining*, pages 128–137. IEEE, 2010.
- Andrija Djuricic, Nebojsa Bozanic, Arjun Ashok, and Rosanne Liu. Extremely simple activation shaping for out-of-distribution detection. In *International Conference on Learning Representations*, 2023.
- Conor Durkan, Artur Bekasov, Iain Murray, and George Papamakarios. nflows: normalizing flows in PyTorch, November 2020. URL <https://doi.org/10.5281/zenodo.4296287>.
- Stanislav Fort, Jie Ren, and Balaji Lakshminarayanan. Exploring the limits of out-of-distribution detection. In *Advances in Neural Information Processing Systems*, 2021.
- Yury Gorishniy, Ivan Rubachev, Valentin Khruikov, and Artem Babenko. Revisiting deep learning models for tabular data. In A. Beygelzimer, Y. Dauphin, P. Liang, and J. Wortman Vaughan, editors, *Advances in Neural Information Processing Systems*, 2021.
- Joe G Greener, Shaun M Kandathil, Lewis Moffat, and David T Jones. A guide to machine learning for biologists. *Nature Reviews Molecular Cell Biology*, 23(1):40–55, 2022.
- Chuan Guo, Geoff Pleiss, Yu Sun, and Kilian Q Weinberger. On calibration of modern neural networks. In *International conference on machine learning*, pages 1321–1330. PMLR, 2017.
- Mehak Gupta, Brennan Gallamoza, Nicolas Cutrona, Pranjal Dhakal, Raphael Poulain, and Rahmatollah Beheshti. An Extensive Data Processing Pipeline for MIMIC-IV. In *Proceedings of the 2nd Machine Learning for Health symposium*, volume 193 of *Proceedings of Machine Learning Research*, pages 311–325. PMLR, 28 Nov 2022.
- Songqiao Han, Xiyang Hu, Hailiang Huang, Minqi Jiang, and Yue Zhao. Adbench: Anomaly detection benchmark. In *Advances in Neural Information Processing Systems*, 2022.
- Matthias Hein, Maksym Andriushchenko, and Julian Bitterwolf. Why relu networks yield high-confidence predictions far away from the training data and how to mitigate the problem. In *Proceedings of the IEEE/CVF Conference on Computer Vision and Pattern Recognition*, pages 41–50, 2019.
- Dan Hendrycks and Kevin Gimpel. A baseline for detecting misclassified and out-of-distribution examples in neural networks. In *International Conference on Learning Representations*, 2017.
- Dan Hendrycks, Steven Basart, Mantas Mazeika, Andy Zou, Joe Kwon, Mohammadreza Mostajabi, Jacob Steinhardt, and Dawn Song. Scaling out-of-distribution detection for real-world settings.

- In *International Conference on Machine Learning*, 2022.
- Rui Huang, Andrew Geng, and Yixuan Li. On the importance of gradients for detecting distributional shifts in the wild. In *Advances in Neural Information Processing Systems*, 2021.
- Alistair EW Johnson, Lucas Bulgarelli, Lu Shen, Alvin Gayles, Ayad Shammout, Steven Horng, Tom J Pollard, Sicheng Hao, Benjamin Moody, Brian Gow, et al. Mimic-iv, a freely accessible electronic health record dataset. *Scientific data*, 10(1):1, 2023.
- Diederik P Kingma and Max Welling. Auto-encoding variational bayes. In *International Conference on Learning Representations*, 2014.
- Shu Kong and Deva Ramanan. Opeengan: Open-set recognition via open data generation. In *Proceedings of the IEEE/CVF International Conference on Computer Vision*, pages 813–822, 2021.
- Kimin Lee, Kibok Lee, Honglak Lee, and Jinwoo Shin. A simple unified framework for detecting out-of-distribution samples and adversarial attacks. 2018.
- Shiyu Liang, Yixuan Li, and R. Srikant. Enhancing the reliability of out-of-distribution image detection in neural networks. In *International Conference on Learning Representations*, 2018.
- Weitang Liu, Xiaoyun Wang, John Owens, and Yixuan Li. Energy-based out-of-distribution detection. In *Advances in neural information processing systems*, 2020.
- Ilya Loshchilov and Frank Hutter. Decoupled weight decay regularization. In *International Conference on Learning Representations*, 2019.
- Sergio Naval Marimont and Giacomo Tarroni. Anomaly detection through latent space restoration using vector quantized variational autoencoders. In *2021 IEEE 18th International Symposium on Biomedical Imaging (ISBI)*, 2021.
- Lotta Meijerink, Giovanni Cinà, and Michele Tonutti. Uncertainty estimation for classification and risk prediction on medical tabular data. *arXiv preprint arXiv:2004.05824*, 2020.
- Alfredo Nazabal, Pablo M Olmos, Zoubin Ghahramani, and Isabel Valera. Handling incomplete heterogeneous data using vaes. *Pattern Recognition*, 107, 2020.
- Giovanna Nicora, Miguel Rios, Ameen Abu-Hanna, and Riccardo Bellazzi. Evaluating pointwise reliability of machine learning prediction. *Journal of Biomedical Informatics*, 127:103996, 2022.
- George Papamakarios, Theo Pavlakou, and Iain Murray. Masked autoregressive flow for density estimation. In *Advances in Neural Information Processing Systems*. Curran Associates, Inc., 2017.
- Tom J Pollard, Alistair EW Johnson, Jesse D Raffa, Leo A Celi, Roger G Mark, and Omar Badawi. The eicu collaborative research database, a freely available multi-center database for critical care research. *Scientific data*, 5(1):1–13, 2018.
- Jie Ren, Stanislav Fort, Jeremiah Liu, Abhijit Guha Roy, Shreyas Padhy, and Balaji Lakshminarayanan. A simple fix to mahalanobis distance for improving near-ood detection. *arXiv preprint arXiv:2106.09022*, 2021.
- Miguel Rios and Ameen Abu-Hanna. Deep kernel learning for mortality prediction in the face of temporal shift. In *Artificial Intelligence in Medicine*, pages 199–208, Cham, 2021. Springer International Publishing.
- Chandramouli Shama Sastry and Sageev Oore. Detecting out-of-distribution examples with gram matrices. In *International Conference on Machine Learning*, pages 8491–8501. PMLR, 2020.
- Syedmostafa Sheikhalishahi, Vevake Balaraman, and Venet Osmani. Benchmarking machine learning models on multi-centre eicu critical care dataset. *Plos one*, 15(7):e0235424, 2020.
- Dimitris Spathis and Stephanie L Hyland. Looking for out-of-distribution environments in critical care: A case study with the eicu database. *arXiv preprint arXiv:2205.13398*, 2022.
- Yiyou Sun and Yixuan Li. Dice: Leveraging sparsification for out-of-distribution detection. In *European Conference on Computer Vision*, 2022.
- Yiyou Sun, Chuan Guo, and Yixuan Li. React: Out-of-distribution detection with rectified activations. In *Advances in Neural Information Processing Systems*, 2021.

- Yiyu Sun, Yifei Ming, Xiaojin Zhu, and Yixuan Li. Out-of-distribution detection with deep nearest neighbors. In *International Conference on Machine Learning*, pages 20827–20840. PMLR, 2022.
- Jeremy Tan, Benjamin Hou, James Batten, Huaqi Qiu, Bernhard Kainz, et al. Detecting outliers with foreign patch interpolation. *Machine Learning for Biomedical Imaging*, 1(April 2022 issue):1–27, 2022.
- Michael E Tipping and Christopher M Bishop. Probabilistic principal component analysis. *Journal of the Royal Statistical Society Series B: Statistical Methodology*, 61(3):611–622, 1999.
- Dennis Ulmer and Giovanni Cinà. Know your limits: Uncertainty estimation with relu classifiers fails at reliable ood detection. In *Uncertainty in Artificial Intelligence*, pages 1766–1776. PMLR, 2021.
- Dennis Ulmer, Lotta Meijerink, and Giovanni Cinà. Trust issues: Uncertainty estimation does not enable reliable ood detection on medical tabular data. In *Proceedings of the Machine Learning for Health NeurIPS Workshop*, volume 136 of *Proceedings of Machine Learning Research*, pages 341–354. PMLR, 11 Dec 2020.
- Joost van Amersfoort, Lewis Smith, Andrew Jesson, Oscar Key, and Yarin Gal. Improving deterministic uncertainty estimation in deep learning for classification and regression. *arXiv preprint arXiv:2102.11409*, 2021.
- Gaël Varoquaux and Veronika Cheplygina. Machine learning for medical imaging: methodological failures and recommendations for the future. *NPJ digital medicine*, 5(1):48, 2022.
- Ashish Vaswani, Noam Shazeer, Niki Parmar, Jakob Uszkoreit, Llion Jones, Aidan N Gomez, Łukasz Kaiser, and Illia Polosukhin. Attention is all you need. In *Advances in neural information processing systems*, 2017.
- Sagar Vaze, Kai Han, Andrea Vedaldi, and Andrew Zisserman. Open-set recognition: A good closed-set classifier is all you need. In *International Conference on Learning Representations*, 2021.
- Haoqi Wang, Zhizhong Li, Litong Feng, and Wayne Zhang. Vim: Out-of-distribution with virtual-logit matching. In *Proceedings of the IEEE/CVF conference on computer vision and pattern recognition*, 2022.
- Jim Winkens, Rudy Bunel, Abhijit Guha Roy, Robert Stanforth, Vivek Natarajan, Joseph R Led-sam, Patricia MacWilliams, Pushmeet Kohli, Alan Karthikesalingam, Simon Kohl, et al. Contrastive training for improved out-of-distribution detection. *arXiv preprint arXiv:2007.05566*, 2020.
- Jingkang Yang, Kaiyang Zhou, Yixuan Li, and Ziwei Liu. Generalized out-of-distribution detection: A survey. *arXiv preprint arXiv:2110.11334*, 2021.
- Jingkang Yang, Pengyun Wang, Dejian Zou, Zitang Zhou, Kunyuan Ding, WENXUAN PENG, Haoqi Wang, Guangyao Chen, Bo Li, Yiyu Sun, Xuefeng Du, Kaiyang Zhou, Wayne Zhang, Dan Hendrycks, Yixuan Li, and Ziwei Liu. OpenOOD: Benchmarking generalized out-of-distribution detection. In *Thirty-sixth Conference on Neural Information Processing Systems Datasets and Benchmarks Track*, 2022.
- Karina Zadorozhny, Patrick Thorat, Paul Elbers, and Giovanni Cinà. Out-of-distribution detection for medical applications: Guidelines for practical evaluation. In *Multimodal AI in healthcare: A paradigm shift in health intelligence*, pages 137–153. Springer, 2022.
- Jingyang Zhang, Jingkang Yang, Pengyun Wang, Haoqi Wang, Yueqian Lin, Haoran Zhang, Yiyu Sun, Xuefeng Du, Kaiyang Zhou, Wayne Zhang, Yixuan Li, Ziwei Liu, Yiran Chen, and Hai Li. Openood v1.5: Enhanced benchmark for out-of-distribution detection. *arXiv preprint arXiv:2306.09301*, 2023a.
- Jinsong Zhang, Qiang Fu, Xu Chen, Lun Du, Zelin Li, Gang Wang, xiaoguang Liu, Shi Han, and Dongmei Zhang. Out-of-distribution detection based on in-distribution data patterns memorization with modern hopfield energy. In *International Conference on Learning Representations*, 2023b.
- David Zimmerer, Peter M Full, Fabian Isensee, Paul Jäger, Tim Adler, Jens Petersen, Gregor Köhler, Tobias Ross, Annika Reinke, Antanas Kascenas, et al. Mood 2020: A public benchmark for out-of-distribution detection and localization on medical images. *IEEE Transactions on Medical Imaging*, 41(10):2728–2738, 2022.

Appendix A. Clinical Variables

Clinical variables selected for each of the eICU and MIMIC-IV datasets are provided in Table 4. These variables are mostly selected as suggested in prior works (Ulmer et al., 2020; Spathis and Hyland, 2022; Rios and Abu-Hanna, 2021). Additionally, we have excluded some time-dependent variables in MIMIC-IV since they are not recorded for most patients. Adding these variables would result in a lot of NaN values. Note that when a dataset is considered as an OOD set for the other one, only available variables for both datasets are included in that experiment.

eICU	MIMIC-IV
<i>• Time-dependent</i>	
pH	pH
Temperature (c)	Temperature
Respiratory Rate	Respiratory rate
O2 Saturation	Oxygen saturation
MAP (mmHg)	Mean blood pressure
Heart Rate	Heart Rate
glucose	Glucose
GCS Total	-
Motor	-
Eyes	-
Verbal	-
FiO2	-
Invasive BP Diastolic	Diastolic blood pressure
Invasive BP Systolic	Systolic blood pressure
<i>• Time-independent</i>	
gender	gender
age	age
ethnicity	-
admissionheight	-
admissionweight	-
-	admission_type
-	first_careunit

Table 4: Clinical time-dependent and time-independent variables used for each of eICU and MIMIC-IV datasets. Corresponding variables are put in the same row, with a dash indicating that the variable is not included in a dataset.

Appendix B. Mortality Prediction

Post-hoc OOD detectors are utilized alongside a prediction model. It is essential that this prediction model is trained well on the ID data (Vaze et al., 2021). Otherwise, the detector would not be able to distinguish IDs and OODs.

Following the guidelines in Gorishniy et al. (2021), we have trained the prediction models for 10 epochs with a batch size equal to 64 and AdamW (Loshchilov and Hutter, 2019) optimizer with a learning rate equal to $1e-3$.

To ensure that our prediction models are trained well, we have measured the AUROC of the mortality prediction task on the test set. Results are presented in Table 5, indicating that models are able to solve the task well. Also, it demonstrates that transformer architecture achieves better performance on this task than MLP and ResNet across both datasets.

Additionally, according to the results in Table 2 and 3, MLP and ResNet in conjunction with distance-based post-hoc detectors can outperform transformers in many cases. This suggests that superior performance as a closed-set classifier on ID data does not necessarily translate to better OOD detection, challenging the claim in Vaze et al. (2021) that better closed-set classifiers lead to improved OOD detection performance.

	eICU	MIMIC-IV
MLP	85.7±1.6	75.6±1.0
ResNet	87.9±0.5	77.3±1.2
FT-Transformer	89.1±0.4	80.1±0.3

Table 5: AUROC of mortality prediction task for MLP, ResNet, and Ft-Transformer architectures on eICU and MIMIC-IV. Results are averaged over 5 runs.

Appendix C. Other Near-OOD Results

Near-OOD results based on age (older than 70 as ID), ethnicity (Caucasian as ID), and first care unit (CVICU as ID) are provided in Table 2. To explore this with other different variables, results for alternate variables are presented in table 6. The variables used in this table are gender (females as ID) and ethnicity (African Americans as ID) for eICU, and gen-

der (females as ID) and admission type (surgical on the same day of admission as ID) for MIMIC-IV.

In eICU, results for both variables indicate an almost random AUC (50%) for all the methods. In MIMIC-IV, gender shows a similar behavior, while for admission type, certain approaches like MDS and AE exhibit marginal superiority over the rest. These results align well with the observations from previous variables in the table 2. First of all, the wide-ranging diversity present in the eICU dataset poses challenges in identifying nearly out-of-distribution sets. Additionally, in scenarios where the difficulty level is not excessively high to the point of random performance, methods like AE and MDS emerge as competitive options. Lastly, the issue of detecting near-OOD samples is still challenging.

Appendix D. FPR@95 Results

In Tables 2 and 3, we presented the results of our analyses, highlighting the performance based on the AUROC. While AUROC serves as a measure of the discriminative capability between novelty scores assigned to ID and OOD data, devoid of any reliance on a predetermined threshold, it would be beneficial to complement this assessment by evaluating the performance at a specific threshold. For this purpose, we have measured the false positive rate at the λ corresponding to the TPR equal to 95% as an acceptable rate for TPR, which is known as FPR@95.

By replacing AUROC with FPR@95 in Tables 2 and 3, we have replicated the corresponding outcomes within Tables 7 and 8. These new tables are in agreement with our conclusions, and if one method has a relatively high AUROC, it would mostly have a relatively low FPR@95. However, it is helpful for comparing methods at a specific threshold. For example, RMDS and KLM applied to an MLP model are achieving similar AUROCs, but RMDS is definitely better at the measured threshold.

Model	Method	eICU				MIMIC-IV			
		Near-OOD(Gender)		Near-OOD(Ethnicity)		Near-OOD(Gender)		Near-OOD(Admission)	
		AUROC	FPR95	AUROC	FPR95	AUROC	FPR95	AUROC	FPR95
Density Based	AE	51.0±0.1	95.0±0.2	47.4±0.4	95.9±0.7	50.2±0.0	94.4±0.1	63.1±1.3	94.0±0.1
	VAE	50.7±0.2	95.0±0.2	47.3±0.4	95.9±0.7	50.2±0.0	94.4±0.1	63.2±1.2	93.9±0.1
	HI-VAE	42.9±0.4	100.0±0.0	46.9±1.6	97.2±1.5	50.2±1.1	94.8±0.4	59.0±18.0	82.1±12.8
	Flow	48.6±0.3	96.3±0.6	48.3±0.4	95.9±0.1	48.2±0.4	95.1±0.5	44.0±4.2	93.9±0.2
	PPCA	51.2±0.2	95.1±0.1	48.1±0.4	95.9±0.2	50.4±0.2	94.4±0.0	61.4±0.5	92.1±1.2
	LOF	53.1±0.3	94.2±0.1	50.2±0.6	94.4±0.1	50.6±0.0	94.1±0.3	60.5±0.5	92.1±0.8
	DUE	50.9±0.6	94.5±0.3	48.7±0.3	95.0±0.2	49.9±0.1	95.4±0.5	57.1±1.0	93.7±1.5
MLP	MDS	48.8±0.1	94.9±0.0	45.4±0.2	95.4±0.4	51.5±0.7	94.4±0.2	60.8±0.2	91.5±1.0
	RMDS	50.9±0.3	94.6±0.3	50.5±0.8	94.8±0.3	48.8±0.8	95.3±0.6	56.1±1.4	91.1±1.8
	KNN	52.1±0.4	94.4±0.3	54.5±0.6	94.5±0.3	48.3±1.0	95.0±0.1	61.6±0.6	93.5±1.2
	VIM	52.2±0.2	94.5±0.1	54.9±0.7	95.2±0.4	48.0±0.7	94.9±0.2	60.5±0.4	91.3±1.1
	SHE	49.0±0.1	95.9±0.3	49.8±0.8	97.3±0.1	50.8±0.2	93.5±0.8	54.0±1.0	92.9±0.9
	KLM	48.8±0.1	94.7±0.2	45.1±0.6	94.1±0.2	51.2±0.2	95.4±0.1	48.5±0.5	91.9±1.3
	OpenMax	52.3±0.2	95.0±0.1	56.5±0.7	94.3±0.1	47.1±0.7	95.5±0.1	57.7±1.3	91.2±0.6
	MSP	52.2±0.2	94.7±0.2	56.8±0.7	94.0±0.0	47.1±0.8	95.5±0.3	57.2±0.9	92.3±1.9
	MLS	52.3±0.2	94.6±0.1	56.9±0.7	94.0±0.1	47.0±0.8	95.2±0.1	57.0±1.0	91.9±2.1
	TempScale	52.2±0.2	94.7±0.2	56.9±0.7	94.0±0.0	47.1±0.8	95.5±0.3	57.0±0.9	92.3±1.9
	ODIN	52.2±0.2	94.7±0.1	56.8±0.7	94.0±0.1	47.1±0.8	95.3±0.2	57.0±1.0	92.3±1.8
	EBO	52.3±0.3	94.9±0.1	56.9±0.7	94.1±0.1	47.0±0.8	95.3±0.0	57.0±1.0	91.8±2.1
	GRAM	51.6±0.6	100.0±0.0	55.0±1.8	100.0±0.0	50.0±0.1	100.0±0.0	49.5±0.8	100.0±0.0
GradNorm	52.2±0.2	94.5±0.2	56.8±0.7	93.8±0.2	47.1±0.7	95.4±0.3	57.0±0.9	90.8±1.1	
ReAct	51.9±0.3	94.9±0.1	56.8±0.7	94.1±0.1	47.2±0.8	95.3±0.0	57.0±1.2	91.8±2.1	
DICE	52.3±0.2	94.2±0.1	56.7±0.8	94.6±0.5	47.1±0.5	95.5±0.3	57.0±1.0	90.3±1.0	
ASH	52.1±0.3	94.8±0.1	56.9±0.4	94.0±0.2	47.3±1.0	95.2±0.1	56.7±2.2	90.6±1.0	
ResNet	MDS	50.4±0.4	95.2±0.2	47.8±0.2	96.2±0.1	50.6±0.1	94.2±0.4	62.2±0.3	92.2±1.0
	RMDS	50.5±0.5	94.8±0.2	50.7±0.6	94.9±0.3	50.2±0.1	94.2±0.1	55.1±0.6	91.9±0.9
	KNN	53.1±0.2	94.4±0.1	51.3±0.6	95.2±0.3	47.9±0.8	94.6±0.3	55.7±1.2	93.9±0.9
	VIM	53.5±0.2	94.7±0.2	51.8±0.8	95.6±0.2	47.4±0.7	95.0±0.1	59.9±0.2	92.0±1.2
	SHE	47.6±0.5	95.7±0.2	45.6±0.6	96.5±0.5	51.7±0.1	94.2±0.1	61.6±1.0	92.6±1.4
	KLM	48.2±0.0	94.1±0.1	47.3±1.0	95.5±0.5	50.6±0.6	95.6±0.5	53.7±0.1	91.4±1.1
	OpenMax	53.7±0.5	94.3±0.1	53.4±1.6	95.0±0.5	46.9±0.6	95.8±0.3	55.2±0.3	92.4±0.9
	MSP	53.7±0.5	93.8±0.2	53.4±1.6	95.0±0.5	46.9±0.7	95.9±0.2	55.2±0.7	91.9±1.1
	MLS	53.7±0.4	94.1±0.3	53.6±1.3	95.0±0.6	46.8±0.6	96.0±0.3	55.2±0.4	91.3±1.1
	TempScale	53.7±0.5	93.8±0.2	53.4±1.6	95.0±0.5	46.9±0.7	95.9±0.2	55.2±0.7	91.9±1.1
	ODIN	53.7±0.5	93.8±0.2	53.4±1.5	95.0±0.4	46.9±0.7	95.8±0.2	55.2±0.7	91.9±1.1
	EBO	53.7±0.4	94.3±0.1	53.6±1.3	94.9±0.7	46.8±0.5	96.1±0.3	55.1±0.4	91.5±0.9
	GRAM	52.5±0.2	100.0±0.0	55.6±1.1	96.3±2.4	50.0±0.0	100.0±0.0	42.6±2.7	100.0±0.0
GradNorm	53.8±0.7	93.8±0.2	55.0±1.2	94.5±0.5	47.0±0.7	95.8±0.2	46.6±1.7	91.4±0.9	
ReAct	53.3±0.3	94.3±0.1	52.6±1.4	95.4±0.6	47.0±0.8	95.9±0.2	58.0±0.3	92.0±1.1	
DICE	52.9±0.2	94.2±0.4	52.6±1.9	94.8±0.3	47.3±0.6	95.2±0.4	51.8±1.4	92.9±0.2	
ASH	53.5±0.6	94.3±0.4	52.8±1.2	95.1±0.6	46.8±0.5	96.1±0.4	53.9±0.5	91.8±1.5	
FT-T	MDS	51.2±0.2	95.2±0.3	52.0±0.7	95.7±0.1	51.6±0.4	94.2±0.1	61.9±0.7	90.1±1.1
	RMDS	51.6±0.8	94.0±0.1	50.8±0.5	94.5±1.0	49.2±0.2	95.6±0.2	53.8±1.0	90.3±1.5
	KNN	52.7±0.3	95.4±0.2	53.1±0.3	95.3±0.4	48.8±0.2	95.0±0.5	63.3±1.1	92.4±1.6
	VIM	53.7±0.3	95.1±0.3	53.7±0.1	95.1±0.2	47.3±0.2	95.4±0.2	62.5±0.3	89.6±1.1
	SHE	49.5±0.2	94.4±0.4	50.5±0.8	94.6±0.2	51.3±0.2	95.2±0.4	55.4±0.6	90.5±1.4
	KLM	47.6±0.6	93.9±0.3	46.0±0.9	94.1±0.3	52.1±0.5	95.5±0.5	46.1±1.0	91.2±1.0
	OpenMax	55.1±0.5	93.8±0.1	55.4±0.1	94.3±0.3	46.3±0.4	95.5±0.1	62.5±0.1	90.2±1.0
	MSP	55.1±0.5	93.8±0.1	55.4±0.1	94.3±0.3	46.4±0.4	95.4±0.3	62.6±0.1	90.2±1.0
	MLS	55.0±0.5	94.0±0.1	55.4±0.1	94.2±0.4	46.4±0.3	95.6±0.1	62.2±0.1	90.4±0.9
	TempScale	55.1±0.5	93.8±0.1	55.4±0.1	94.3±0.3	46.4±0.4	95.4±0.3	62.6±0.1	90.2±1.0
	ODIN	55.1±0.5	93.8±0.1	55.4±0.1	94.3±0.3	46.4±0.4	95.4±0.3	62.6±0.1	90.3±1.0
	EBO	55.0±0.5	94.0±0.1	55.4±0.1	94.6±0.3	46.4±0.3	95.6±0.3	62.2±0.2	90.9±1.2
	GRAM	54.3±1.2	94.4±0.2	54.7±0.8	94.6±0.2	46.6±0.9	95.7±0.3	55.8±5.4	89.9±1.5
GradNorm	53.5±0.1	93.8±0.1	51.1±4.3	94.6±0.4	47.2±1.3	95.4±0.3	49.3±5.8	90.5±1.1	
ReAct	54.9±0.4	94.0±0.1	55.6±0.1	94.3±0.3	46.4±0.4	95.4±0.4	61.7±0.8	90.9±1.4	
DICE	54.9±0.5	94.3±0.5	55.3±0.1	94.4±0.2	46.6±0.5	95.5±0.2	61.6±0.2	90.4±0.9	
ASH	54.7±0.6	94.3±0.2	51.4±1.6	95.1±0.5	46.7±0.2	95.4±0.3	54.8±2.2	90.5±1.4	

Table 6: Comparing OOD detection methods in the *near-OOD* setting, with performance evaluated through AUROC and FPR@95. In eICU, distinguishing variables are gender (females as ID) and ethnicity (African Americans as ID). In MIMIC-IV, distinguishing variables are gender (females as ID) and admission type (surgical on the same day of admission as ID). Results are averaged over 3 runs. For each model, the best value in each column is shown in bold, and distance-based post-hoc approaches are distinguished with a lighter color.

Model	Method	eICU			MIMIC-IV		
		Far-OOD	Near-OOD (Eth)	Near-OOD (Age)	Far-OOD	Near-OOD (FCU)	Near-OOD (Age)
Density Based	AE	17.5±5.3	93.3±1.6	94.3±0.2	0.2±0.3	72.7±11.5	90.7±0.7
	VAE	22.5±7.4	93.3±1.5	94.6±0.2	0.2±0.3	71.9±11.8	90.7±0.8
	HI-VAE	83.4±1.5	100.0±0.0	100.0±0.0	99.9±0.1	44.5±21.9	90.9±6.9
	Flow	0.0±0.0	89.6±4.9	94.7±0.4	35.9±39.2	96.8±1.1	93.5±1.0
	PPCA	15.5±4.3	91.5±3.5	93.8±0.3	0.3±0.3	76.7±9.8	92.0±0.6
	LOF	17.4±2.3	92.8±2.4	95.5±0.2	3.5±0.6	78.4±5.4	91.9±0.4
	DUE	80.9±6.1	94.3±1.6	94.5±0.1	7.6±2.5	88.6±3.2	91.1±0.4
MLP	MDS	62.7±6.6	91.1±2.6	94.6±0.3	4.3±3.2	85.2±2.2	92.5±0.6
	RMDS	90.3±5.0	94.7±1.5	95.7±0.2	60.0±29.2	89.8±5.3	95.0±0.1
	KNN	73.3±13.1	93.5±3.7	95.9±0.2	81.9±18.8	78.8±3.8	93.4±0.6
	VIM	84.9±7.3	94.2±1.8	95.4±0.5	9.5±6.4	82.3±1.1	93.0±0.8
	SHE	87.8±1.1	94.4±1.4	94.0±0.8	26.6±15.7	93.3±1.5	96.1±0.4
	KLM	93.3±1.1	94.7±1.5	95.8±0.2	82.2±16.5	90.8±5.1	94.2±0.5
	OpenMax	93.8±3.9	95.9±1.4	95.9±0.1	70.4±24.4	87.0±2.1	94.7±0.9
	MSP	94.7±3.4	97.2±2.0	95.9±0.2	99.1±1.0	91.6±6.5	94.7±0.7
	MLS	94.6±3.6	95.4±1.3	96.0±0.2	98.3±1.6	87.8±3.9	94.5±0.6
	TempScale	94.7±3.4	95.9±1.1	95.9±0.2	99.1±1.0	89.1±6.4	94.7±0.7
	ODIN	94.7±3.4	95.4±1.3	95.9±0.3	98.9±1.1	88.0±4.0	94.6±0.8
	EBO	94.5±3.7	95.4±1.3	96.0±0.2	96.8±3.1	87.8±3.9	94.8±0.6
	GRAM	99.4±0.3	98.1±3.0	100.0±0.0	100.0±0.0	98.7±2.1	100.0±0.0
	GradNorm	95.3±2.7	95.5±1.2	95.8±0.2	99.1±0.8	88.4±3.9	94.6±0.6
	ReAct	93.6±2.4	95.4±1.0	96.0±0.2	72.5±17.4	87.7±3.8	94.8±0.6
DICE	95.8±2.5	95.3±0.9	95.0±0.2	97.8±3.2	88.2±3.8	94.2±1.1	
ASH	94.3±3.7	95.9±0.9	95.8±0.4	97.2±2.7	88.7±2.7	94.7±0.3	
ResNet	MDS	14.0±1.9	90.5±3.3	94.0±0.2	0.4±0.4	77.4±9.2	92.1±0.9
	RMDS	93.0±4.1	95.0±1.8	95.1±0.1	54.9±32.1	88.2±8.1	94.7±0.4
	KNN	39.4±7.0	88.3±3.3	95.3±0.1	32.9±17.0	93.0±2.2	93.4±0.6
	VIM	28.7±2.2	89.8±2.0	94.5±0.2	1.1±1.1	81.3±2.2	91.8±0.8
	SHE	54.2±4.7	94.8±0.6	94.2±0.2	0.5±0.6	79.2±7.2	93.3±0.4
	KLM	90.9±3.2	95.0±0.7	95.1±0.3	88.5±8.6	89.0±5.7	93.9±0.1
	OpenMax	85.2±4.6	95.8±1.5	95.7±0.6	62.6±31.8	88.8±6.4	93.6±0.2
	MSP	89.3±2.9	94.5±0.9	95.5±0.2	97.1±3.5	89.6±7.1	94.7±0.3
	MLS	86.2±4.4	94.3±1.2	95.7±0.5	88.3±8.6	88.5±7.4	94.2±0.1
	TempScale	89.3±2.9	94.5±0.9	95.5±0.2	97.1±3.5	89.6±7.1	94.7±0.3
	ODIN	89.3±2.9	94.5±0.9	95.5±0.2	97.0±3.5	89.6±7.0	94.8±0.3
	EBO	84.8±5.5	94.3±1.2	95.7±0.8	86.9±10.1	87.7±8.9	93.3±0.6
	GRAM	99.8±0.3	95.2±1.2	100.0±0.0	100.0±0.0	99.5±0.4	100.0±0.0
	GradNorm	94.7±2.4	94.7±1.7	95.6±0.2	99.1±1.1	91.5±6.1	94.8±0.2
	ReAct	79.7±6.8	94.0±1.4	95.5±0.6	60.1±32.3	81.2±4.8	93.0±0.5
DICE	95.2±1.4	95.9±0.9	95.4±0.2	98.6±2.6	90.9±6.2	93.3±0.6	
ASH	81.2±5.9	93.3±2.8	95.7±0.6	86.5±17.5	88.9±7.0	93.4±0.7	
FT-T	MDS	61.1±14.6	89.7±4.3	94.3±0.5	29.5±11.5	73.8±7.9	94.2±0.9
	RMDS	91.1±4.9	93.1±1.6	95.6±0.1	64.4±25.9	88.5±6.8	94.4±0.3
	KNN	53.2±13.4	91.8±2.0	94.7±0.2	38.4±22.3	70.7±10.5	93.9±0.1
	VIM	57.6±11.5	90.7±4.3	94.6±0.0	18.1±2.1	76.1±1.6	92.5±0.6
	SHE	84.7±2.6	93.2±1.8	95.1±0.3	52.5±17.1	83.8±5.9	96.7±0.2
	KLM	89.5±5.1	92.8±1.4	95.2±0.3	70.4±8.8	86.8±9.0	95.7±0.5
	OpenMax	80.4±1.9	93.8±1.9	95.2±0.1	78.6±17.3	78.3±3.7	94.3±0.3
	MSP	80.4±2.0	93.5±1.6	95.3±0.2	80.2±15.2	77.8±4.4	95.0±0.2
	MLS	80.7±2.0	93.4±1.6	95.3±0.1	82.5±10.9	77.3±3.9	95.1±0.2
	TempScale	80.4±2.0	93.5±1.6	95.3±0.2	80.2±15.2	77.8±4.4	95.0±0.2
	ODIN	80.3±2.0	93.5±1.6	95.3±0.2	80.1±15.2	77.8±4.2	95.0±0.2
	EBO	80.9±2.1	93.3±1.6	95.2±0.1	83.1±9.5	78.1±3.2	94.6±0.3
	GRAM	87.7±2.7	93.6±2.3	95.0±0.3	67.6±18.8	77.6±7.8	94.5±0.3
	GradNorm	87.2±2.1	92.0±3.2	95.3±0.2	78.1±14.4	86.0±6.5	95.0±0.2
	ReAct	81.0±2.0	94.5±2.3	95.2±0.2	82.4±9.2	80.1±1.3	94.2±0.3
DICE	80.1±2.1	93.0±2.2	94.9±0.1	57.8±7.8	80.2±4.4	92.4±0.8	
ASH	81.2±2.6	92.6±2.1	95.3±0.1	92.1±8.0	80.5±5.5	95.3±0.6	

Table 7: Comparing OOD detection methods in the *far-OOD* and *near-OOD* settings using eICU and MIMIC-IV datasets, with performance evaluated through FPR@95. This Table is similar to Table 2, but assesses FPR@95 instead of utilizing AUROC. FCU and Eth stand for first care unit and ethnicity as the variables utilized for constructing the ID/OOD sets. Results are averaged over 5 runs. For each model, the best value in each column is shown in bold, and distance-based post-hoc approaches are distinguished with a lighter color.

Model	Method	eICU			MIMIC-IV		
		$\mathcal{F}=10$	$\mathcal{F}=100$	$\mathcal{F}=1000$	$\mathcal{F}=10$	$\mathcal{F}=100$	$\mathcal{F}=1000$
Density Based	AE	47.1±3.9	25.4±3.7	22.0±4.1	51.6±3.8	35.3±3.2	28.5±4.2
	VAE	47.9±4.0	25.6±3.7	22.1±4.2	51.5±3.7	35.1±3.1	28.4±4.1
	HI-VAE	94.9±0.2	94.7±0.2	94.7±0.5	94.9±0.4	94.5±0.6	94.1±0.9
	Flow	60.2±7.2	36.8±7.4	26.5±5.2	82.1±3.1	62.6±3.3	44.6±2.1
	PPCA	46.6±2.7	25.8±4.4	22.8±5.0	50.7±3.3	35.0±3.1	28.6±4.2
	LOF	35.4±3.6	23.9±4.3	21.5±4.4	46.4±3.2	32.6±3.7	27.5±3.5
	DUE	78.2±4.6	47.9±2.5	25.8±3.9	83.1±2.5	53.0±4.7	37.2±2.7
MLP	MDS	67.9±5.4	42.3±3.2	24.5±4.0	67.1±4.7	43.0±5.1	32.6±3.6
	RMDS	77.5±0.9	50.6±2.6	30.7±4.0	87.9±2.0	66.2±2.4	45.4±2.1
	KNN	82.8±8.4	73.1±12.8	67.9±15.8	79.9±6.1	61.7±14.6	53.0±18.5
	VIM	86.4±2.2	77.1±2.6	69.0±5.1	79.0±9.1	59.8±16.8	51.0±17.6
	SHE	77.1±4.7	48.0±2.8	24.5±4.0	77.5±1.7	48.4±6.2	35.0±4.1
	KLM	86.3±8.5	77.5±17.9	71.2±22.7	88.6±4.8	74.5±11.6	65.5±15.9
	OpenMax	83.9±0.8	60.6±2.4	42.1±4.1	91.3±1.1	74.5±3.1	55.1±6.7
	MSP	94.0±0.4	95.6±0.6	98.4±1.0	93.7±0.6	96.0±0.6	97.1±0.7
	MLS	94.1±0.4	95.8±0.9	98.5±0.9	93.4±0.8	93.8±2.1	93.2±3.1
	TempScale	94.0±0.4	95.6±0.6	98.4±0.9	93.8±0.6	96.1±0.6	97.2±0.6
	ODIN	94.0±0.4	95.6±0.6	98.4±1.0	93.7±0.6	96.0±0.5	97.1±0.6
	EBO	94.2±0.4	95.7±1.1	98.5±0.9	93.3±1.1	93.4±2.5	92.9±3.3
	GRAM	98.0±1.7	98.7±0.8	99.9±0.0	99.9±0.1	99.9±0.1	99.9±0.1
	GradNorm	94.2±0.5	96.0±0.4	98.9±0.7	94.3±0.5	96.9±0.4	97.7±0.6
ReAct	92.4±2.3	91.8±4.0	91.4±5.3	92.5±1.2	89.7±3.0	86.8±4.6	
DICE	93.1±0.6	93.7±0.9	95.5±2.0	93.2±0.4	94.6±0.9	96.0±2.0	
ASH	94.2±0.5	95.6±0.8	98.1±1.0	93.6±0.8	93.4±2.3	92.6±3.0	
ResNet	MDS	57.7±4.5	26.6±4.5	20.6±4.9	60.9±2.3	39.7±2.7	30.7±3.0
	RMDS	87.2±2.7	64.5±6.3	39.1±6.0	91.6±1.7	70.7±2.9	47.9±4.0
	KNN	69.4±4.9	41.4±6.1	33.0±6.5	70.3±3.3	46.7±0.7	35.5±1.8
	VIM	60.9±4.8	26.9±4.1	19.7±4.3	65.8±0.8	42.4±3.5	31.9±3.7
	SHE	68.3±3.2	34.4±2.8	20.4±3.0	71.4±4.6	44.2±2.9	32.3±2.7
	KLM	88.4±1.3	72.7±8.0	58.0±14.1	90.9±1.3	74.8±4.9	63.7±8.5
	OpenMax	83.0±1.0	64.0±6.0	42.9±9.6	87.2±3.7	69.7±2.1	61.0±13.3
	MSP	91.4±2.5	93.6±1.6	97.7±0.4	90.6±3.1	94.1±1.7	97.5±0.2
	MLS	90.8±1.6	92.0±1.3	94.6±2.2	89.9±3.6	89.8±5.4	89.1±7.6
	TempScale	91.4±2.5	93.6±1.6	97.8±0.4	90.7±3.1	94.1±1.7	97.5±0.2
	ODIN	91.4±2.5	93.6±1.6	97.7±0.4	90.5±3.0	94.1±1.6	97.5±0.3
	EBO	90.6±1.5	91.8±1.5	94.4±2.3	89.7±3.8	89.0±6.1	88.8±8.2
	GRAM	98.6±1.6	99.9±0.1	100.0±0.0	99.8±0.2	99.9±0.1	99.9±0.1
	GradNorm	95.0±0.4	98.2±1.0	99.4±0.4	94.2±0.4	97.5±0.7	98.4±0.2
ReAct	83.7±5.9	71.9±14.7	64.8±19.4	86.1±7.3	75.7±15.0	70.2±19.0	
DICE	94.3±1.4	97.4±0.5	99.2±0.6	90.4±3.7	92.6±2.6	95.6±1.2	
ASH	91.1±1.0	91.5±1.9	93.7±3.1	90.3±3.4	89.7±5.2	89.1±7.6	
FT-T	MDS	81.6±1.3	48.1±4.1	28.0±4.9	82.3±3.6	52.5±2.4	38.6±4.7
	RMDS	91.9±2.3	78.7±10.4	64.2±17.7	94.1±0.3	79.0±8.2	58.2±11.6
	KNN	83.6±1.8	53.4±5.3	29.8±5.6	85.5±2.3	55.0±1.7	39.7±4.6
	VIM	81.9±2.8	48.7±3.5	26.6±3.0	85.5±4.3	54.1±2.1	40.5±4.5
	SHE	88.2±2.5	63.0±6.6	41.6±4.4	91.2±1.3	68.4±2.9	43.3±5.3
	KLM	91.0±1.8	79.5±4.4	60.9±9.7	93.2±0.9	81.8±3.6	76.5±7.2
	OpenMax	91.2±1.9	80.7±4.8	60.6±9.2	94.2±0.5	83.9±4.8	75.0±13.1
	MSP	91.0±1.4	79.2±2.5	58.8±5.3	94.7±0.4	88.1±3.0	74.8±7.9
	MLS	91.2±1.0	80.4±3.7	61.0±7.7	94.5±0.5	87.9±5.8	79.2±13.8
	TempScale	91.0±1.4	79.2±2.5	58.8±5.3	94.7±0.4	88.0±3.0	74.8±7.9
	ODIN	90.9±1.4	79.0±2.4	58.4±5.1	94.8±0.4	88.1±3.0	74.6±7.7
	EBO	91.6±0.8	82.0±5.1	63.7±9.0	94.4±0.7	88.1±6.0	80.3±14.3
	GRAM	94.1±0.6	89.8±4.7	79.9±8.3	95.1±0.3	88.9±2.8	77.9±7.0
	GradNorm	91.3±1.4	78.6±4.5	58.3±6.7	94.5±0.5	87.2±3.7	74.1±8.1
ReAct	91.8±0.7	82.9±3.9	65.5±6.7	94.1±0.8	87.2±5.3	78.3±11.8	
DICE	88.3±1.1	66.9±2.3	45.1±2.7	92.6±1.6	69.5±2.4	48.3±3.8	
ASH	91.6±0.7	81.0±4.5	61.0±6.9	94.6±0.6	88.2±5.0	80.4±13.6	

Table 8: Comparing OOD detection methods in the *synthesized-OOD* setting using eICU and MIMIC-IV datasets, with performance evaluated through FPR@95. This Table is similar to Table 3, but assesses FPR@95 instead of utilizing AUROC. In this setting, one feature is multiplied by a specific factor \mathcal{F} to construct an OOD sample. For each model and factor we display the average performance, calculated over 100 resampling of the feature and 5 different initializations of the model. For each model, the best value in each column is shown in bold, and distance-based post-hoc approaches are distinguished with a lighter color.